


RESEARCH

Open Access



Investigation on geothermal binary-flashing cycle employing zeotropic mixtures as working fluids

Lingbao Wang^{1,2,3}, Xianbiao Bu^{1,2,3} and Huashan Li^{1,2,3*} 

*Correspondence:

lihs@ms.giec.ac.cn

¹ Guangzhou

Institute of Energy
Conversion, Chinese
Academy of Sciences,
Guangzhou 510640, China
Full list of author information
is available at the end of the
article

Abstract

The binary-flashing cycle (BFC) is supposed to be a promising technology for geothermal recovery due to the full use of geofluid. For further performance improvement, the potential of using mixtures of a hydrocarbon and a retardant in the BFC system is investigated. R245fa is selected as a retardant and blended with R600 to form zeotropic mixtures. With the thermal efficiency (η_{th}), exergy efficiency (η_{ex}), net power output per ton geofluid (PRW), and exergy destruction rate (E_d) as evaluation indexes, the flowsheet modeling and optimization are conducted to explore the optimal compositions and operating parameters. It is revealed the optimal mass fraction of R600/R245fa is 0.44/0.56, at which the flammability of R600 is suppressed, the global warming potential (GWP) of R245fa is reduced. The maximum η_{ex} and PRW are higher than those of component fluids. The maximum E_d occurs in the heat exchanger, which should be optimized. The recommended generation pressures are 1200–1430, 1240–1480, 1220–1460, and 1170–1420 kPa, respectively, for R600 mass fraction of 0.2, 0.4, 0.6, and 0.8. In addition, the flashing temperature is also optimized. Although the mixtures do not always yield superior performance, it is still beneficial to apply the mixtures to the BFC system through systematic consideration of safety and environmental friendliness.

Keywords: Binary-flashing cycle, Zeotropic mixtures, Geothermal energy, R245fa, R600, Optimum performance

Introduction

The accelerated energy demand causes growing consumption of fossil fuels and massive discharge of pollutants, which promotes the development of renewable energy utilization. Among other renewable energy sources, the geothermal energy has the advantages of reliability, sustainability, high capacity factor and less ecological effect (Liu et al. 2017). Over 70% of the geothermal sources available in the world are of low-enthalpy with the temperature lower than 150 °C (Franco and Vaccaro 2014). As an efficient technology in the exploitation of the low–medium temperature geothermal energy, Organic Rankine Cycle (ORC) systems have drawn great attention (Pollet et al. 2018; Sadeghi et al. 2016).

Nevertheless, the thermal efficiency of the ORC system is generally less than 12% (Basaran and Ozgerer 2013), which is a serious obstacle for further application. It is not well-optimized from the view of thermodynamics. One major disadvantage of the ORC

is the complete evaporation of working fluid accounting for large amount of the total input heat. As a consequence, the evaporation temperature and pressure are relatively low, leading to lower power output. As a modification, the binary-flashing cycle (BFC) is proposed to be an efficient system to overcome such a problem (Edrisi and Michaelides 2013; Liu et al. 2018; Michaelides and Scott 1984; Michaelides 2016; Shi and Michaelides 1989; Wang et al. 2016, 2018; Yuan and Michaelides 1993). The working fluid is not evaporated completely in the BFC system. And lesser heat rate is demanded in the evaporation process. As a consequence, the evaporation temperature and pressure are higher than those in the ORC system. The liquid-state working fluid from the evaporator is flashed in the flashing tank to produce more steam at a lower temperature. And an additional amount of power is obtained.

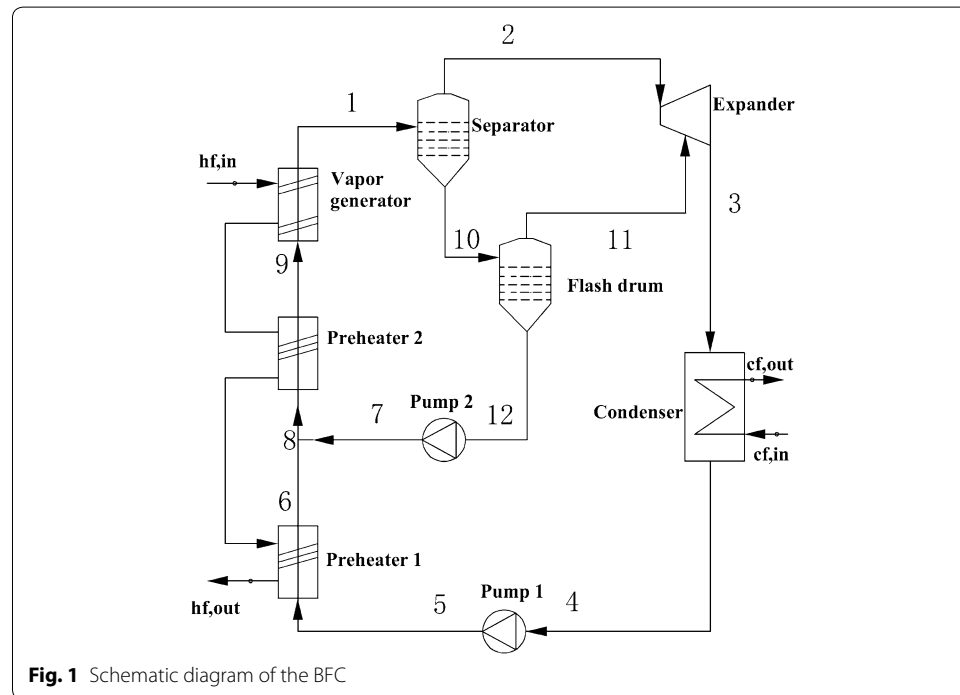
Up to date, the research focusing on the BFC is very limited. Michaelides and Scott (1984) analyzed the geothermal BFC system employing freon, ammonia, and isobutene as working fluids. It is indicated the BFC system would produce 20% more power than the ORC system. The superior thermodynamic performance of the BFC system is also found in Shi and Michaelides (1989). Yuan and Michaelides (1993) found that BFC system may provide up to 25% more work than the conventional ORC system under the optimum operation conditions. Edrisi and Michaelides (2013) compared several pure working fluids, including normal butane, isobutane, hexane, pentane, refrigerant-114, and ammonia, employed in the BFC system. It is suggested that among the six working fluids, hexane and pentane appear to be a better choice. Michaelides (2016) found that the overall entropy production is reduced in the BFC system, which is proposed to be the future cycle for geothermal power generation system. Wang et al. (2018) proposed a BFC system with a regenerator to recover the waste heat of the working fluid at the turbine exit. And the working fluid selection was conducted. Wang et al. (2016) carried out the comparison among the ORC, double-evaporator ORC and BFC. The thermal efficiency, power output per ton geothermal brine, and reinjection temperature of geothermal brine were selected as the evaluation indicators. Liu et al. (2018) investigated the performance characteristics and conducted the working selection for the BFC. It is indicated that there exists an optimum generation temperature and flashing temperature at which the system achieves the optimal performance.

A brief literature survey reveals that all the investigations on the BFC system focused solely on pure working fluids. The pure working fluids in BFC have a large entropy generation during evaporation and condensation process, due to the isothermal behavior. Fortunately, the issue can be partially solved by zeotropic mixtures, which exhibits non-isothermal characteristics during heat transfer process. Great efforts have been devoted to the using of the zeotropic mixtures in the ORC systems. The superiority of the zeotropic mixtures applying in the ORC system has been generally recognized (Dong et al. 2018; Harby 2017; Zhai et al. 2018).

However, none of the previous work investigated the BFC system using the zeotropic mixtures as a working fluid. To fill up this research gap, the objective of the present study is to verify the potential benefits of the zeotropic mixtures in the BFC system. Due to the excellent thermal performance and zero ozone depletion potential (ODP), R245fa is recommended as the working fluid in the ORC system (Feng et al. 2017; Imran et al. 2014; Liu et al. 2013). And it is frequently used in the experimental study (Dong et al.

Table 1 Thermophysical properties of the selected pure working fluids

Fluid	Molecular mass (kg/kmol)	Critical temperature (°C)	Critical pressure (kPa)	Normal boiling point (°C)	GWP	Flammability
R245fa	134.05	154.01	3651.00	15.14	1030	Non flammable
R600	58.12	151.98	3796.00	-0.49	~20	Flammable



2017; Galloni et al. 2015; Guillaume et al. 2017). However, it has relatively high global warming potential (GWP), which has certain unfavorable effects on the environment. The hydrocarbons are attractive due to the highest thermal performance and cheapness (Li et al. 2017; Song and Gu 2015). However, the flammability and chemical instability of the hydrocarbons limit their practical applications (Budisulistyo and Krumdieck 2015). In the present study, a blending of hydrocarbons and R245fa is proposed. Furthermore, the mixtures have the potential to suppress the flammability of the hydrocarbon and reduce the GWP of R245fa. The thermophysical properties of R245fa and R600 are listed in Table 1. The first law efficiency, the second law efficiency, and power capability per unit ton geofluid are chosen as the evaluation criteria.

BFC system description

The BFC system mainly consists of two preheaters, a vapor generator, a separator, a high-pressure expander, a flash drum, a low-pressure expander, a condenser, and two working fluid pumps. A schematic diagram of the BFC system is depicted in Fig. 1. For simplicity, only one expander is depicted. The geothermal brine flows into the vapor generator and heats up the working fluid. The working fluid is partially vaporized at a predetermined dryness fraction. The gas–liquid mixture is sent to the separator, where the gas is

separated from the mixture and flows into the high-pressure expander to produce work. The remaining liquid is sent to the flash drum, where it is flashed at a lower temperature and pressure. An additional quantity of vapor is produced and fed to the low-pressure expand to produce more work. The remaining liquid working fluid released from the flash drum is pumped to the preheater 2 and is heated by the geothermal brine from the vapor generator. The working fluid from the high-pressure and low-pressure expand is condensed to liquid state in the condenser by the cooling water. Subsequently, the working fluid is pumped to preheater 1, where the working fluid is heated by the geothermal brine from preheater 2. Then the left geothermal brine is re-injected to the reservoir. Finally, the working fluid from preheater 2 is sent to the vapor generator to continue cycle operation.

Thermodynamic model

The model is established on the typical simplifying assumptions as follows (Dai et al. 2016):

1. All processes are operated under steady-state conditions;
2. Pressure loss and heat dissipation in all components and pipelines are negligible except for the expander and pump;
3. Friction losses, kinetic energy, and potential energy are neglected;
4. Saturated liquid is assumed at the condenser exit;
5. The irreversibility related to the separator is ignored;
6. The geothermal brine has the properties of pure water.

Based on the assumptions above, a set of basic equations and the specific thermodynamic processes are described as follows.

The evaporator contains three components, i.e., preheater 1, preheater 2, and vapor generator.

For the preheater 1

$$Q_{\text{Pre1}} = m_{\text{hf}} c_{\text{p,hf}} (T_{\text{p,2}} - T_{\text{hf,out}}) = m_5 (h_6 - h_5) \quad (1)$$

$$m_5 = m_1 (X_{\text{gen}} + (1 - X_{\text{gen}}) X_{\text{fsh}}) \quad (2)$$

For the preheater 2

$$Q_{\text{Pre2}} = m_{\text{hf}} c_{\text{p,hf}} (T_{\text{p,1}} - T_{\text{p,2}}) = m_{\text{wf}} (h_9 - h_8) \quad (3)$$

$$m_2 = m_1 X_{\text{gen}} \quad (4)$$

For the vapor generator

$$Q_{\text{gen}} = m_{\text{hf}} c_{\text{p,hf}} (T_{\text{hf,in}} - T_{\text{p,1}}) = m_2 (h_1 - h_9) \quad (5)$$

The total heat transfer rate absorbed by the evaporator can be written by:

$$Q_{\text{evp}} = Q_{\text{Pre1}} + Q_{\text{Pre2}} + Q_{\text{gen}} \quad (6)$$

where Q is the heat transfer rate, kW; m is the mass flow rate, kg/s; c_p is the specific heat capacity, kJ/(kg K); T is the temperature, °C; h is the specific enthalpy, kJ/kg; X is the dryness fraction; the subscripts “hf”, “wf”, “Pre1”, “Pre2”, “in”, “gen” and “fsh” denote geothermal brine, working fluid, preheater 1, preheater 2, vapor generator and flash drum, respectively; the subscripts “in” and “out” represent the inlet and exit of the components, respectively. The subscript numbers of the equations presented in this section represent the working state points in the cycle as shown in Fig. 1.

For the separator

$$m_1 = m_2 + m_{10} \quad (7)$$

For the flash drum

$$m_{10} = m_{11} + m_{12} \quad (8)$$

$$m_{11} = m_{10}X_{\text{fsh}} + m_{12} \quad (9)$$

For the high-pressure expander

The power produced by the expander is given by:

$$W_{\text{exp}} = m_2(h_2 - h_3) + m_{11}(h_{11} - h_3) = m_2(h_2 - h_{2,s})\eta_{\text{exp}} + m_{11}(h_{11} - h_{11,s})\eta_{\text{exp}} \quad (10)$$

For the condenser

$$Q_{\text{con}} = m_{\text{cf}}c_{p,\text{cf}}(T_{\text{cf,out}} - T_{\text{cf,in}}) = m_3(h_3 - h_4) \quad (11)$$

$$m_3 = m_2 + m_{11} = m_{\text{wf}}X_{\text{gen}} + m_{\text{wf}}(1 - X_{\text{gen}})X_{\text{fsh}} \quad (12)$$

where the subscripts “con” and “cf” denote the condenser and cooling water, respectively.

For the pump 1

The required power of the pump is given by:

$$W_{\text{pup1}} = m_5(h_5 - h_4) = m_5(h_{4,s} - h_4) / \eta_{\text{pup}} \quad (13)$$

$$m_5 = m_4 = m_3 \quad (14)$$

where the subscript “pup” denotes the working fluid pump.

For the pump 2

$$W_{\text{pup2}} = m_{12}(h_7 - h_{12}) = m_{12}(h_{12,s} - h_{12}) / \eta_{\text{pup}} \quad (15)$$

Evaluation indicators

The net power output is expressed by:

$$W_{\text{net}} = W_{\text{exp}} - W_{\text{pup1}} - W_{\text{pup2}} \quad (16)$$

where the subscript “net” represents net output.

The thermal efficiency is written by:

$$\eta_{\text{th}} = W_{\text{net}} / Q_{\text{tot}} \quad (17)$$

PRW is defined as the ratio of net power output to unit ton geothermal brine, which reflects the power capability per ton geothermal brine.

$$\text{PRW} = W_{\text{net}} / m_{\text{wat}} \quad (18)$$

where m_{wat} is the mass flow rate of geothermal brine, t/h.

The exergy efficiency is defined as the ratio of the net output power to input exergy:

$$\eta_{\text{ex}} = W_{\text{net}} / E_{\text{in}} \quad (19)$$

The input exergy is expressed by:

$$E_{\text{in}} = m_{\text{hf}} c_{\text{p,hf}} \left[(T_{\text{hf,in}} - T_{\text{hf,out}}) - T_0 \ln \left(\frac{T_{\text{hf,in}}}{T_{\text{hf,out}}} \right) \right] \quad (20)$$

The exergy destruction rate of the components can be expressed as follows:

$$E_{\text{D,exp}} = T_0 (m_3 s_3 - m_2 s_2 - m_{11} s_{11}) \quad (21)$$

$$E_{\text{D,con}} = T_0 m_4 \left[(s_4 - s_3) - \frac{(h_4 - h_3)}{T_{\text{m,con}}} \right] \quad (22)$$

$$E_{\text{D,pup1}} = T_0 m_5 (s_5 - s_4) \quad (23)$$

$$E_{\text{D,Pre1}} = T_0 m_6 \left[(s_6 - s_5) - \frac{(h_6 - h_5)}{T_{\text{m,Pre1}}} \right] \quad (24)$$

$$E_{\text{D,pup2}} = T_0 m_{12} (s_7 - s_{12}) \quad (25)$$

$$E_{\text{D,Pre2}} = T_0 m_9 \left[(s_9 - s_8) - \frac{(h_9 - h_8)}{T_{\text{m,Pre2}}} \right] \quad (26)$$

$$E_{\text{D,gen}} = T_0 m_1 \left[(s_1 - s_9) - \frac{(h_1 - h_9)}{T_{\text{m,gen}}} \right] \quad (27)$$

$$E_{\text{D,fsh}} = T_0 (m_{11} s_{11} + m_{12} s_{12} - m_{10} s_{10}) \quad (28)$$

The total exergy destruction rate is expressed by:

$$E_{\text{D,tot}} = E_{\text{D,exp}} + E_{\text{D,con}} + E_{\text{D,pup1}} + E_{\text{D,Pre1}} + E_{\text{D,pup2}} + E_{\text{D,Pre2}} + E_{\text{D,gen}} + E_{\text{D,fsh}} \quad (29)$$

where E_{D} is the exergy destruction rate, kW; T_0 is the ambient temperature, °C; the subscript “m” represents the thermodynamic mean value.

It should be noted that the typical flashing temperature is approximately equal to the average of the generation and condensation temperature (Edrisi and Michaelides 2013).

$$T_{\text{fsh}} = (T_{\text{gen}} + T_{\text{con}})/2 \quad (30)$$

There exists a practical flashing temperature in the BFC system. To investigate the influence of flashing temperature on the system performance conveniently, a symbol is defined as temperature difference between the practical flashing temperature and the typical flashing temperature:

$$\delta T = T_{\text{fsh_rea}} - T_{\text{fsh}} \quad (31)$$

where $T_{\text{fsh_rea}}$ is the practical flashing temperature, °C.

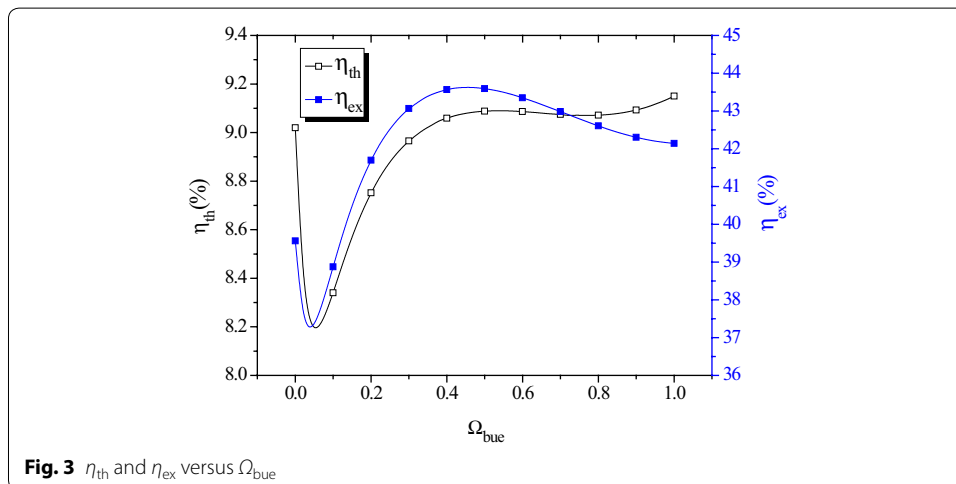
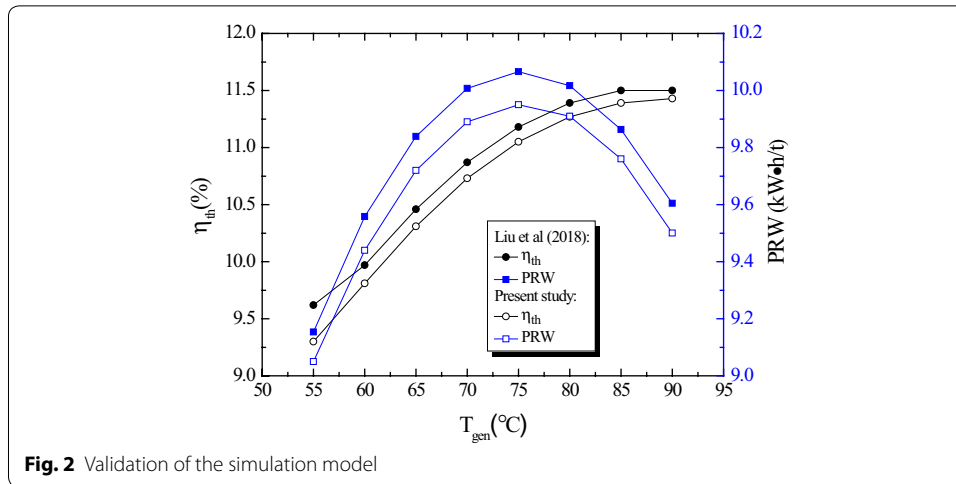
Based on the above assumptions and equations, simulations and optimizations of zeotropic fluid composition are carried out by MATLAB software. All of the properties of the working fluids are acquired from REFPROP 9.1 (Lemmon et al. 2013). The operating conditions and parameters are listed in Table 2. Note that the analysis is performed by varying one parameter at a time while keeping the others as the typical values given in Table 2.

Model validation

Due to the lack of studies on BFC system running with the zeotropic mixtures, the validation of the present calculating program is conducted based on the results of pure working fluid. The η_{th} and PRW against T_{gen} are calculated by the present model and compared with the research investigated by Liu et al. (2018) under the same working condition using R245fa. The comparison result is depicted in Fig. 2. It can be observed that the maximum deviations of the η_{th} and PRW between the present solutions and results from Liu et al. (2018) are less than 3.3% and 1.5%, respectively. It exhibits a good agreement between the developed model and published reference values. The present model can be applied to predict the BFC system performance using the zeotropic mixtures within the acceptable error range.

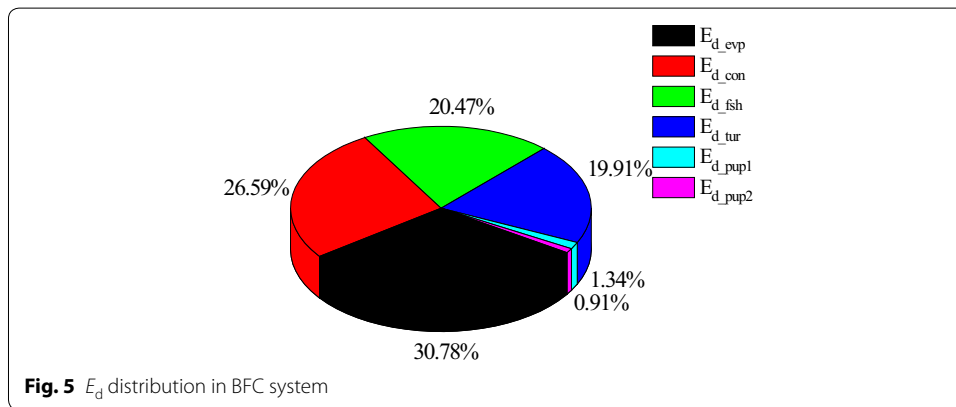
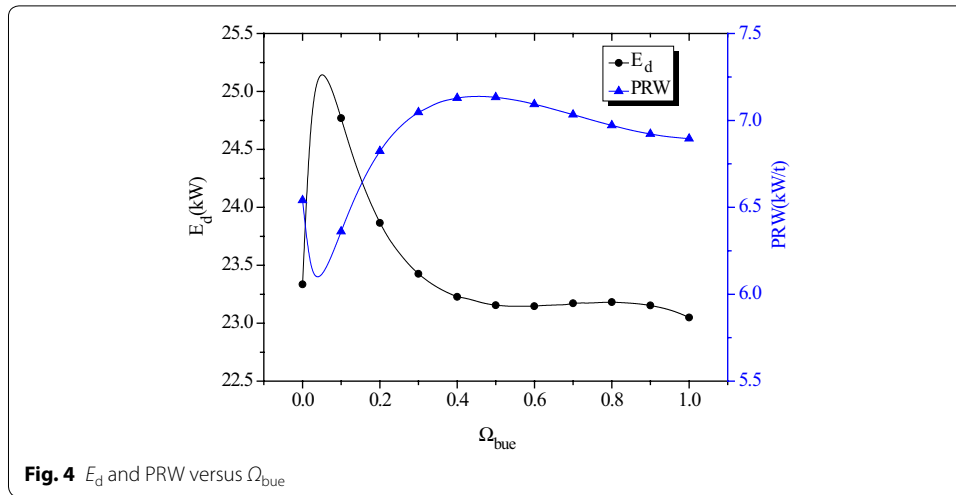
Table 2 Operating conditions and parameters

Parameters	Typical value	Ranges
Geothermal brine inlet temperature, °C	120	–
Geothermal brine inlet pressure, kPa	300	–
Geothermal brine flow rate, kg/s	1	–
Cooling water inlet temperature, °C	20	–
Cooling water inlet pressure, kPa	100	–
Condensation temperature, °C	30	–
Generation pressure, kPa	1400	1000–1700
Flashing temperature, °C	T_{fsh}	$(T_{\text{fsh}} - 10) - (T_{\text{fsh}} + 10)$
Pinch point temperature difference, °C	5	
Isentropic efficiency of expander	0.85	
Isentropic efficiency of pump	0.80	
Ambient temperature, °C	20 °C	



Results and discussion

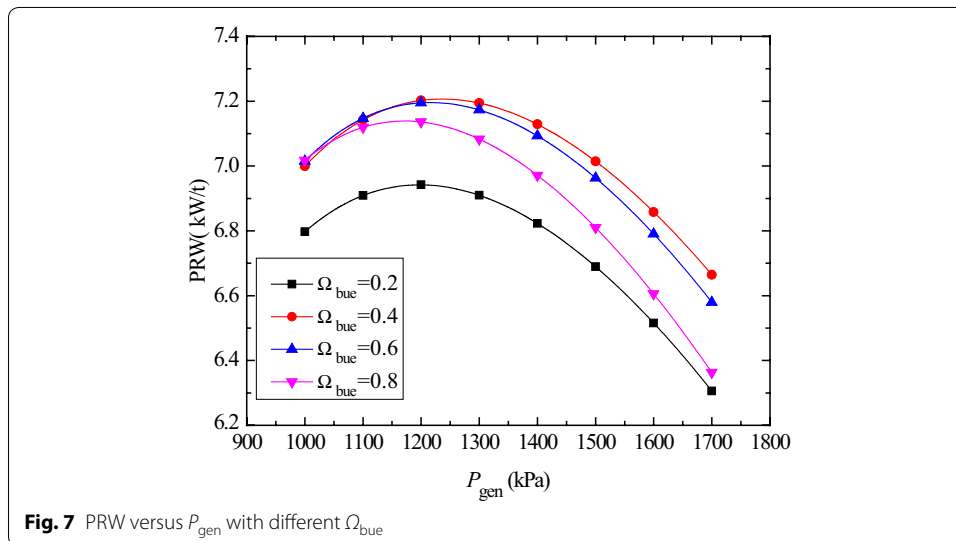
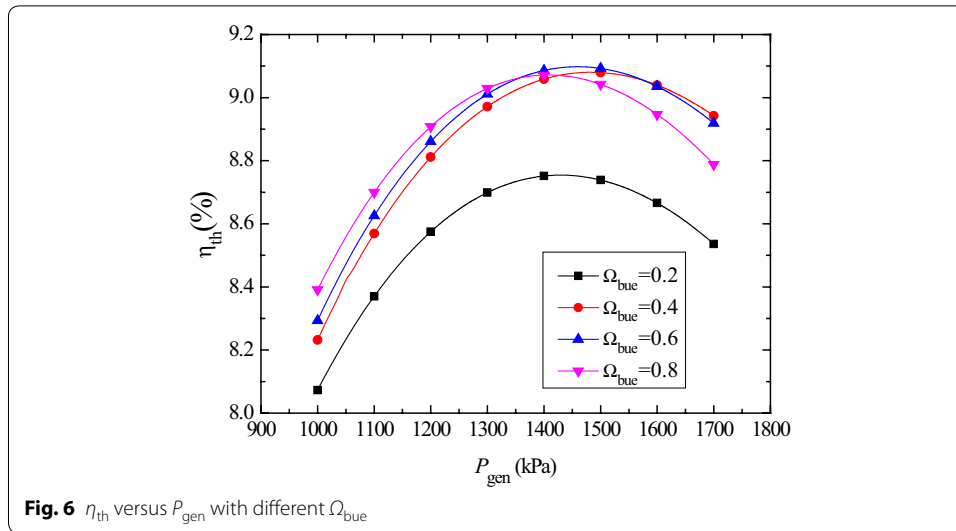
The Ω_{bue} represents the mass fraction of R600 in the mixtures. The effect of Ω_{bue} on the η_{th} and η_{ex} is illustrated in Fig. 3. It is obvious that the η_{th} and η_{ex} firstly decrease and then increase with the increment of Ω_{bue} . And the η_{th} and η_{ex} present remarkable similar variation tendency. The η_{th} of the mixtures remains higher than that of R245fa until Ω_{bue} exceeds 0.36. The η_{ex} reaches the maximum of 43.62% at 0.44 for Ω_{bue} . When the Ω_{bue} is larger than 0.24, the mixtures always yield higher η_{ex} than their component fluids. Specific attention should be paid to the rebound and fluctuation in η_{th} as Ω_{bue} approaches to 1. The mixtures play a more important role in raising η_{ex} than η_{th} . Zabetakis (1965) studied the flammability envelopes of the mixtures of hydrocarbons and nonflammable working fluids. It is indicated that 0.3 volume fraction of retardants is adequate to make mixture nonflammable. The molecular weight of R245fa (134.05 g/mol) is much larger than that of R600 (58.12 g/mol). When the mass fraction of R245fa is 0.49, it is enough to suppress the flammability of the mixtures. Shu et al. (2014) proposed the mass fraction of retardants ranging from 0.3 to



0.7 in the ORC system, with the hydrocarbons and refrigerant retardants mixtures as working fluid. According to Ding (1997), the GWP of the mixtures is weighted by the mass fraction of each component. The blending with a certain amount of R600 is beneficial to reduce the GWP relative to R245fa employed alone. That is to say, when the η_{th} and η_{ex} obtain the optimal values, the R245fa and R600 mixtures bestow with merits of both fluids sans their flammability and large GWP demerits.

Figure 4 shows the variations of E_d and PRW with respect to Ω_{bue} . The PRW firstly decreases, then increases, and at last decreases slowly. The mixtures always present higher PRW in the range of 0.24–0.94 for Ω_{bue} . The PRW achieve the maximum (7.14) at 0.44 for Ω_{bue} . It is quite clear that the η_{ex} and PRW get the maximal value simultaneously at 0.44 for Ω_{bue} . The maximal PRW of the mixtures is 9.2% and 3.5% higher than that of R245fa and R600, respectively. While an opposite trend is exhibited for E_d . The E_d increases rapidly, then decreases drastically, and at last tends to stable and fluctuates. The Ω_{bue} should be not less than 0.32 to avoid larger E_d .

The E_d distribution in the BFC system with Ω_{bue} of 0.44 is illustrated in Fig. 5. Note that the E_d of the separator is ignored. From the distribution pie chart, it is observed the maximum E_d occurs in evaporator, followed by the condenser, flash drum, expander, pump 1 and pump 2 in sequence. The E_d of the heat exchangers, i.e.,



evaporator and condenser, accounts for 57.37% of the total E_d . Therefore, more attention should be paid to cut down the E_d of the heat exchangers. The study on heat transfer mechanism and heat exchanger design should be enhanced. The E_d of the two working fluid pumps is both very low, accounting for only 1.34% and 0.91% of the E_d , respectively. That is to say the working fluid pump has little impact on the system performance.

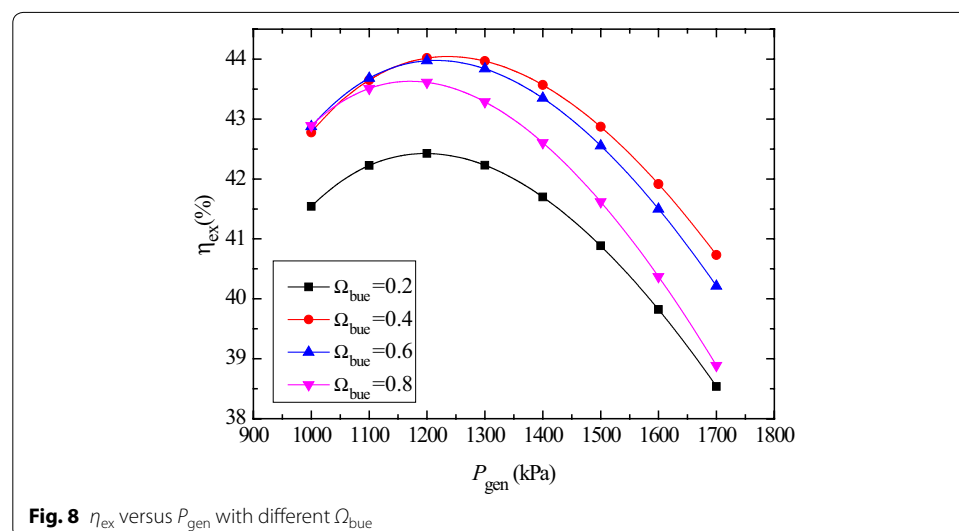
The variation of η_{th} with P_{gen} under different Ω_{bue} is presented in Fig. 6. For all the Ω_{bue} examined, η_{th} firstly rises dramatically, reaches the maximum, and then declines slowly with the increased P_{gen} . Under a specific working condition, i.e., a certain flashing temperature and condensation temperature, the rise in P_{gen} causes the specific enthalpy drop across the turbine increasing, while it will raise the mass flow rate of the mixtures. With the two conflicting influences, an optimum P_{gen} exists and makes the η_{th} obtain the maximum value, which is well in conformity with Edrisi and Michaelides (2013). The

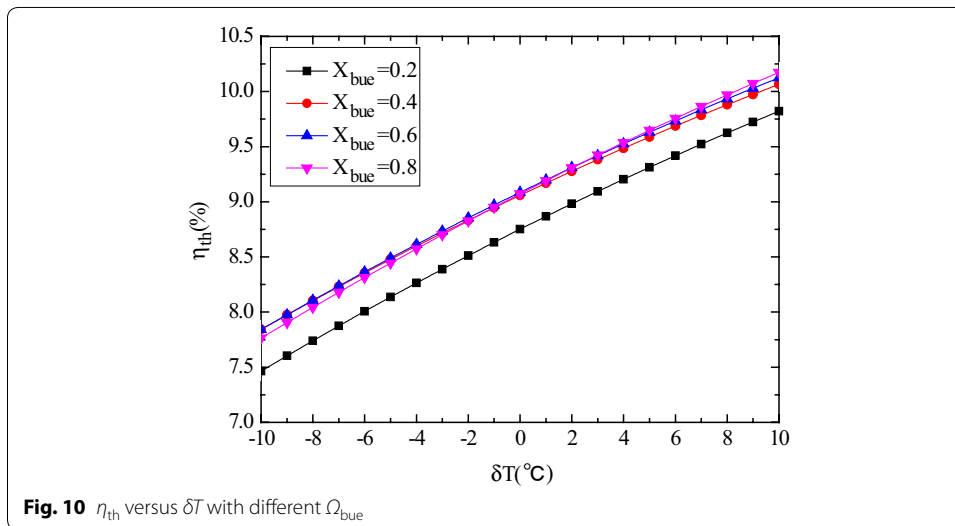
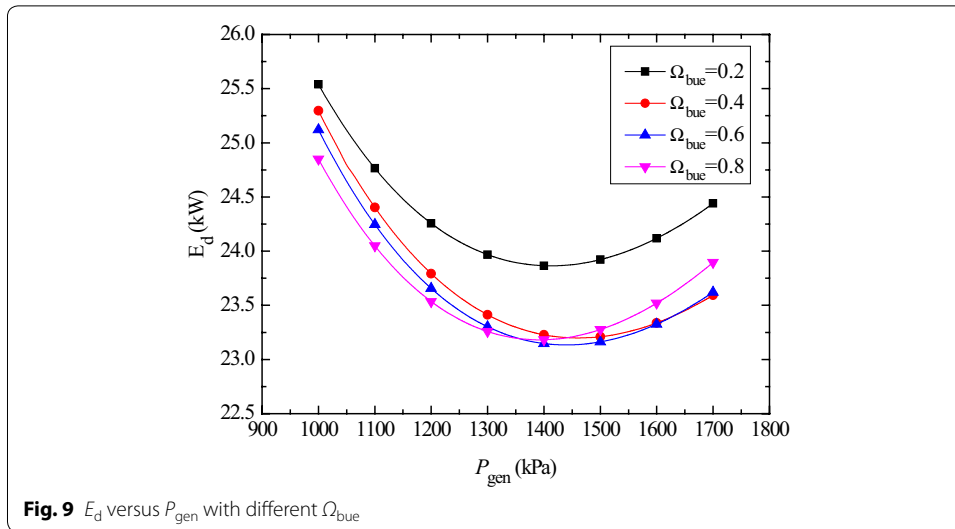
optimum P_{gen} is 1430, 1480, 1460, and 1420 kPa for Ω_{bue} of 0.2, 0.4, 0.6 and 0.8, respectively. The optimum P_{gen} is in a narrow range for different Ω_{bue} .

The variation of PRW with P_{gen} under different Ω_{bue} is depicted in Fig. 7. As can be seen, PRW emerges a curve first going up slowly then down remarkably. The optimum P_{gen} is 1200, 1240, 1220 and 1170 kPa for Ω_{bue} of 0.2, 0.4, 0.6, and 0.8, respectively. It is obvious that the corresponding optimum P_{gen} of the maximum PRW is much lower than that of maximum η_{th} under the same Ω_{bue} . The discharge temperature of the geothermal brine increases with increase in P_{gen} , leading to the drop of the input heat flux in the evaporator. Initially, the growth rate of η_{th} is larger than the decrease rate of input heat flux in the evaporator, PRW is increased. It can be discovered from Fig. 6 that when P_{gen} is less than the corresponding optimum P_{gen} , the growth rate of η_{th} is decreased. When the growth rate of η_{th} is less than the decrease rate of input heat flux in the evaporator, PRW is decreased. In Fig. 7, when P_{gen} is larger than the corresponding optimal P_{gen} of maximum η_{th} , the PRW decreases remarkably. The η_{th} and PRW cannot reach the maximum simultaneously. It is imperative to conduct multi-objective optimization to acquire the most suitable P_{gen} . The recommended P_{gen} are 1200–1430, 1240–1480, 1220–1460, and 1170–1420 kPa, respectively, for Ω_{bue} of 0.2, 0.4, 0.6, and 0.8.

The variation of η_{ex} with P_{gen} under different Ω_{bue} is presented in Fig. 8. The η_{ex} presents a similar variation tendency with the PRW when P_{gen} increases. Although there both exist optimum P_{gen} for the η_{th} and η_{ex} , the variation trend has significant discrepancies. The optimum P_{gen} of the η_{ex} is the same with that of PRW with the same Ω_{bue} . The variation of E_d with P_{gen} under different Ω_{bue} is presented in Fig. 9. As expected, as shown in Fig. 9, the variation tendency of the E_d runs opposite with that of PRW. The optimum P_{gen} are 1410, 1460, 1440, and 1390 kPa at 0.2, 0.4, 0.6, and 0.8 for Ω_{bue} , respectively, which are slightly lower than those of maximum η_{th} .

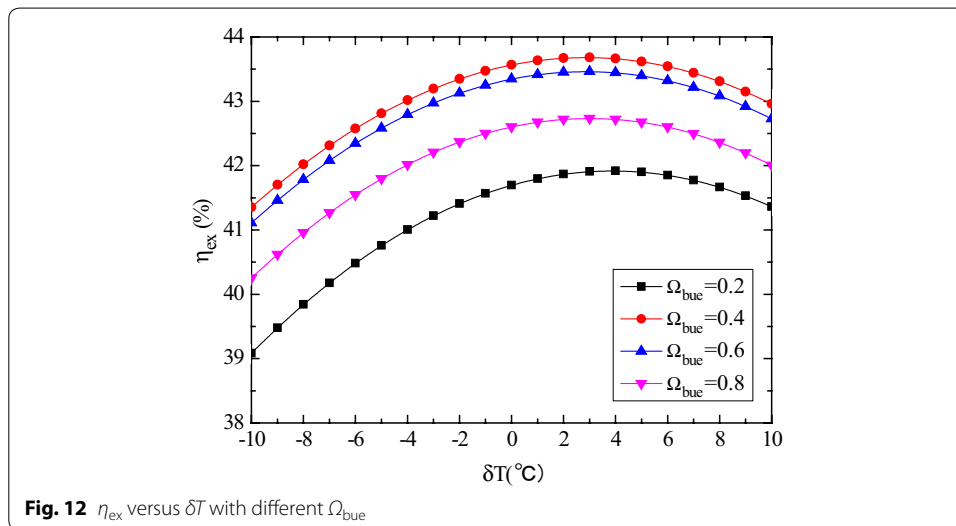
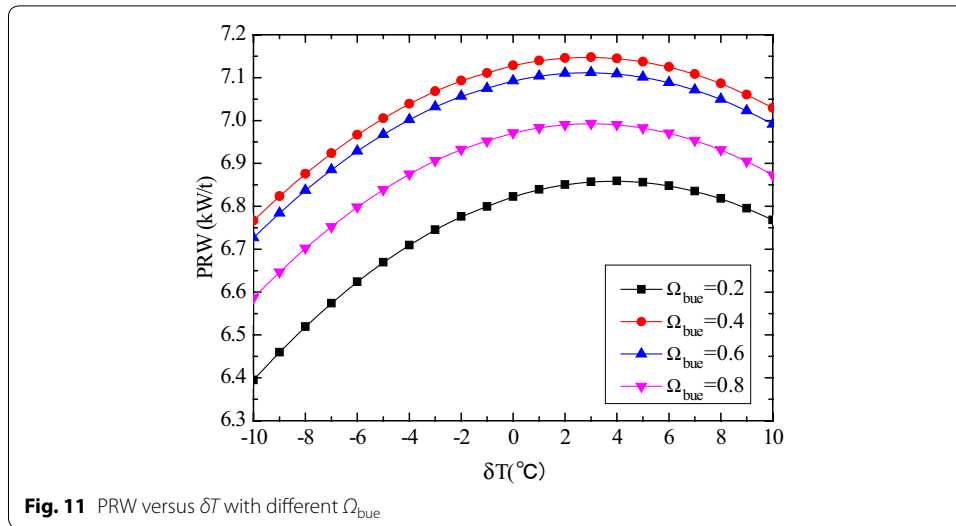
Due to the adding of the separator and flashing tanking, the BFC system is equivalent to the coupling of the ORC system and organic working fluid flashing system. An additional T_{fsh} is required to be optimized. Figure 10 exhibits the variation of η_{th} with δT under different Ω_{bue} . It can be observed that under various Ω_{bue} , the η_{th} keeps going up





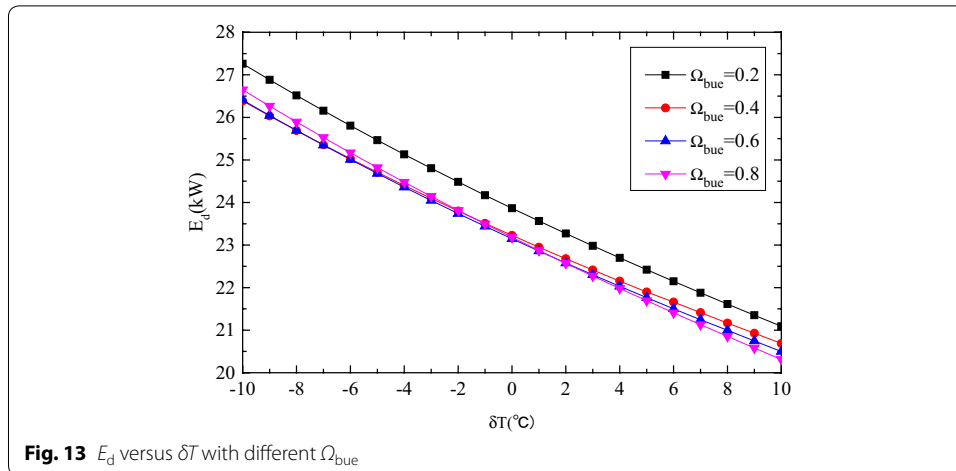
almost linearly with the increasing of δT . The increase in δT means a raise of T_{fish} . It corresponds to enlarge the T_{fish} of the organic working fluid flashing system with the ORC system unchanged. It will be easy to understand the increase in the η_{th} . It is conceivable that when the T_{fish} is equal to T_{gen} , the η_{th} reach the maximum, and the BFC system becomes to the ORC system. Take $\Omega_{bue}=0.4$ as example, the η_{th} is improved by 28.3% with δT of 10 °C than that of -10 °C.

Figure 11 illustrates the effect of δT on PRW with different Ω_{bue} . It can be seen that the PRW initially increases and attains maximum value then decreases with the rising Ω_{bue} . The increase in T_{fish} causes the decline of the mass flow rate of working fluid vapor, and rise of specific enthalpy drop across the turbine, under a specific working condition, i.e., a certain P_{gen} and T_{con} . With the interaction between the two effects, an optimum T_{fish} exists and makes the PRW obtain the maximum value, which is well in conformity with



Edrisi and Michaelides (2013). For all the Ω_{bue} investigated, the PRW has a peak value with δT of 3 °C.

Figure 12 presents the influence of δT on the η_{ex} with different Ω_{bue} . The η_{ex} firstly increases and then decreases for all Ω_{bue} . There exists a δT at which the η_{ex} achieve the maximum. The optimum δT s at 0.2, 0.4, 0.6 and 0.8 for Ω_{bue} are 4, 3, 3, and 3 °C, respectively. As sated above, W_{net} first rises and then declines. It is known that the raising T_{fsh} leads to the increase in geothermal brine reinjection temperature, which results in the decrease in input exergy. So the η_{ex} increases significantly firstly. Afterward, because the decreased range of W_{net} is larger than that of input exergy, η_{ex} is decreased. By comprehensive analysis of Figs. 6 and 7, there exists an optimum δT of 3 °C at which the PRW and η_{ex} achieve the maximum simultaneously.



The influence of δT on E_d is displayed in Fig. 13, and it can be seen that the E_d almost decreases linearly with the increase in δT . The increase in δT leads to the decrease in input heat of evaporator, and the degree of irreversibility in the heat transfer process is decreased. The E_d drops by 22.5% on average when δT increases from -10 to 10 °C.

Conclusions

In the present study, a geothermal BFC system employing the zeotropic working fluid is explored theoretically. One of the contributions is the potential of applying R245fa and R600 mixtures in the BFC system. The following conclusions can be drawn:

1. The η_{th} of the mixtures remains higher than that of R245fa until Ω_{bue} exceeds 0.36. And the maximum η_{th} is slightly smaller than that of R600. The maximum η_{ex} and PRW are higher than the component fluids, and reach the maximum simultaneously at 0.44 for Ω_{bue} . In order to avoid larger E_d , the X_{bue} should be not less than 0.32. The optimal Ω_{bue} is 0.44, at which the flammability of R600 is suppressed, and the GWP of R245fa is reduced.
2. The maximum exergy destruction rate of the BFC system occurs in evaporator, followed by the condenser, flash drum, expander, pump 1 and pump 2 in sequence. The exergy destruction rate in the heat exchangers accounts for 57.37% of the total exergy destruction rate.
3. For all the Ω_{bue} examined, η_{th} , PRW and η_{ex} firstly increase, then decline with the rising P_{gen} . And the variation of the E_d presents the opposite trend. The η_{ex} and PRW attain superior under the same P_{gen} . The η_{th} and E_d gain the optimal values simultaneously on the whole. The recommended P_{gen} are 1200–1430, 1240–1480, 1220–1460, and 1170–1420 kPa at 0.2, 0.4, 0.6 and 0.8 for Ω_{bue} .
4. The η_{th} almost increases linearly with the increasing δT under various Ω_{bue} . The η_{ex} and PRW firstly increase and then decrease and reach the maximum under the same δT (3 °C). The E_d almost decreases linearly with the raising of δT .

Generally speaking, the mixtures may not always show outstanding thermal performance. Nevertheless, the mixtures can overcome the shortcomings of the component and extend the selection range of working fluid from the viewpoint of environmental impacts and safety aspects. The application of R245fa/R600 mixtures applying the BFC system is beneficial.

Finally and as future work, with the maximum η_{th} , maximum PRW and minimum capitalized cost as objective function, Ω_{bue} , P_{gen} , δT , and perhaps other operating parameters as decision variables, multi-objective optimization will be conducted. What is more, the economic feasibility of the zeotropic mixtures employing in BFC system will be carried out.

Abbreviations

List of symbols

c_p : specific heat capacity (kJ/kg K⁻¹); E_D : exergy destruction rate (kW); E_{in} : input exergy (kW); h : specific enthalpy (kJ/kg); m : mass flow rate (kg/s); P : pressure (kPa); Q : heat transfer rate (kW); T : temperature (°C); PRW: power output per unit geothermal brine mass flow rate (kW/t); qu : quality; W : work (kW).

Greek

η : efficiency; δ : difference value.

Subscripts

0: ambient condition; 1, 2, ..., 12: state points; cf: cooling water; con: condenser; evp: evaporator; exp: expander; fsh: flash tank; gen: vapor generator; hf: heat source fluid; in: inlet; m: thermodynamic mean value; net: net output; out: outlet; Pre1: preheater 1; Pre2: preheater 2; pup1: pump 1; pup2: pump 2; s: isentropic process; tot: total; wat: water; wf: working fluid.

Acronyms

BFC: binary flashing cycle; ODP: ozone depletion potential; ORC: Organic Rankine Cycle; GWP: global warming potential.

Acknowledgements

We express our gratitude to W.B. Ma for technical support while writing the MATLAB program.

Authors' contributions

LW built the workflow of the BFC, designed the model, run all simulations on MATLAB, and drafted the manuscript. XB provided guidance and insight into evaluating the results and his experience in the use of MATLAB. HL provided guidance and insight into evaluating the results and helped drafting the manuscript. All authors contributed to the preparation of the manuscript and the interpretation of the data and model results. All authors read and approved the final manuscript.

Funding

The authors gratefully acknowledge the financial supports provided by the National Key R&D Program of China (No. 2018YFB1501805), and Natural Science Foundation of Guangdong Province (No. 2016A030313174), and National Natural Science Foundation of China (No. 41972314).

Availability of data and materials

The datasets used and/or analyzed during the current study are available from the corresponding author on reasonable request.

Competing interests

The authors declare that they have no competing interests.

Author details

¹ Guangzhou Institute of Energy Conversion, Chinese Academy of Sciences, Guangzhou 510640, China. ² CAS Key Laboratory of Renewable Energy, Guangzhou 510640, China. ³ Guangdong Provincial Key Laboratory of New and Renewable Energy Research and Development, Guangzhou 510640, China.

Received: 19 October 2019 Accepted: 26 November 2019

Published online: 05 December 2019

References

- Basaran A, Ozgerer L. Investigation of the effect of different refrigerants on performances of binary geothermal power plants. *Energy Convers Manag.* 2013;76:483–98.
- Budisulistyo D, Krumdieck S. Thermodynamic and economic analysis for the pre-feasibility study of a binary geothermal power plant. *Energy Convers Manag.* 2015;103:639–49.

- Dai XY, Shi L, An QS, Qian WZ. Screening of hydrocarbons as supercritical ORCs working fluids by thermal stability. *Energy Convers Manag.* 2016;126:632–7.
- Ding GL. Alternatives to CFCs for refrigeration appliances in Germany and TEWI. Shanghai: Annual conference of Shanghai Refrigeration Society; 1997. p. 153–7.
- Dong JQ, Zhang XH, Wang JZ. Experimental investigation on heat transfer characteristics of plate heat exchanger applied in organic Rankine cycle (ORC). *Appl Therm Eng.* 2017;112:1137–52.
- Dong BS, Xu GQ, Li TT, Quan YK, Wen J. Thermodynamic and economic analysis of zeotropic mixtures as working fluids in low temperature organic Rankine cycles. *Appl Therm Eng.* 2018;132:545–53.
- Edrisi BH, Michaelides EE. Effect of the working fluid on the optimum work of binary-flashing geothermal power plants. *Energy.* 2013;50:389–94.
- Feng YQ, Hung TC, He YL, Wang Q, Wang S, Li BX, Lin JR, Zhang WP. Operation characteristic and performance comparison of organic Rankine cycle (ORC) for low-grade waste heat using R245fa, R123 and their mixtures. *Energy Convers Manag.* 2017;144:163.
- Franco A, Vaccaro M. Numerical simulation of geothermal reservoirs for the sustainable design of energy plants: a review. *Renew Sustain Energy Rev.* 2014;30:987–1002.
- Galloni E, Fontana G, Staccone S. Design and experimental analysis of a mini ORC (organic Rankine cycle) power plant based on R245fa working fluid. *Energy.* 2015;90:768–75.
- Guillaume L, Legros A, Desideri A, Lemort V. Performance of a radial-inflow turbine integrated in an ORC system and designed for a WHR on truck application: an experimental comparison between R245fa and R1233zd. *Appl Energy.* 2017;186:408–22.
- Harby K. Hydrocarbons and their mixtures as alternatives to environmental unfriendly halogenated refrigerants: an updated overview. *Renew Sustain Energy Rev.* 2017;73:1247–64.
- Imran M, Park BS, Kim HJ, Dong HL, Usman M, Heo M. Thermo-economic optimization of regenerative organic Rankine cycle for waste heat recovery applications. *Energy Convers Manag.* 2014;87:107–18.
- Li L, Ge YT, Luo X, Tassou SA. Experimental investigations into power generation with low grade waste heat and R245fa Organic Rankine Cycles (ORCs). *Appl Therm Eng.* 2017;115:815–24.
- Liu Q, Duan Y, Yang Z. Performance analyses of geothermal organic Rankine cycles with selected hydrocarbon working fluids. *Energy.* 2013;63:123–32.
- Liu XM, Wei M, Yang LN, Wang X. Thermo-economic analysis and optimization selection of ORC system configurations for low temperature binary-cycle geothermal plant. *Appl Therm Eng.* 2017;125:153–64.
- Liu X, Li HS, Bu XB, Wang LB, Xie N, Zeng J. Performance characteristics and working fluid selection for low-temperature binary flashing cycle. *Appl Therm Eng.* 2018;141:51–60.
- Michaelides EE. Future directions and cycles for electricity production from geothermal resources. *Energy Convers Manag.* 2016;107:3–9.
- Michaelides EE, Scott GJ. A binary-flashing geothermal power plant. *Energy.* 1984;9:323–31.
- Lemmon EW, Huber MH, McLinden MO. REFPROP, NIST Standard Reference Database 23. Version 9.1, USA. 2013.
- Pollet M, Gosselin L, Dallaire J, Mathieu Potvin F. Optimization of geothermal power plant design for evolving operating conditions. *Appl Therm Eng.* 2018;134:118–29.
- Sadeghi M, Nemat A, Ghavimi A, Yari M. Thermodynamic analysis and multi-objective optimization of various ORC (organic Rankine cycle) configurations using zeotropic mixtures. *Energy.* 2016;109:791–802.
- Shi H, Michaelides EE. Binary dual-flashing geothermal power plants. *Int J Energy Res.* 1989;13:127–35.
- Shu GQ, Gao YY, Tian H, Wei HQ, Liang XY. Study of mixtures based on hydrocarbons used in ORC (Organic Rankine Cycle) for engine waste heat recovery. *Energy.* 2014;74:428–38.
- Song G, Gu CW. Analysis of ORC (Organic Rankine Cycle) systems with pure hydrocarbons and mixtures of hydrocarbon and retardant for engine waste heat recovery. *Appl Therm Eng.* 2015;89:693–702.
- Wang YX, Wang LB, Li HS, Bu XB. Thermodynamic calculation and optimization of geothermal power generation in Ganzhi. *J Harbin Eng Univ.* 2016;37:873–7.
- Wang LB, Bu XB, Li HS, Wang HZ, Ma WB. Working fluids selection for flashing organic rankine regeneration cycle driven by low-medium heat source. *Environ Prog Sustain Energy.* 2018;37:1201–9.
- Yuan Z, Michaelides EE. Binary-flashing geothermal power plants. *J Energy Resour Technol.* 1993;115:232–6.
- Zabetakis MG. Flammability characteristics of combustible gases and vapor. Washington DC: Bureau of Mines; 1965.
- Zhai HX, An QS, Shi L. Zeotropic mixture active design method for organic Rankine cycle. *Appl Therm Eng.* 2018;129:1171–80.

Publisher's Note

Springer Nature remains neutral with regard to jurisdictional claims in published maps and institutional affiliations.